SLAC-PUB-1671
November 1975
(T/E)

MUON PROTON SCATTERING*

R. F. Mozley

Stanford Linear Accelerator Center
Stanford University, Stanford, California USA

I report results of an examination of the final states in a muon proton scattering experiment performed with the SLAC two-meter streamer chamber.

Participants in the experiment were:

SLAC	U. C. SANTA CRUZ	
K. Bunnell	D. Cheng	A. Seiden
M. Duong-van	D. Dorfan	T. Schalk
R. Mozley	S. Flatte	A. Grillo
A. Odian	C. Heusch	B. Lieberman
F. Villa	G. Luxton	L. Moss
L. Wang	H. Meyer	C. del Papa

The experiment was performed using a beam of 14 GeV/c positive muons incident on a 40 cm liquid hydrogen target inside a 2 meter streamer chamber accepting almost the entire 4π final state solid angle. (See Fig. 1.) A trigger was caused by any particle

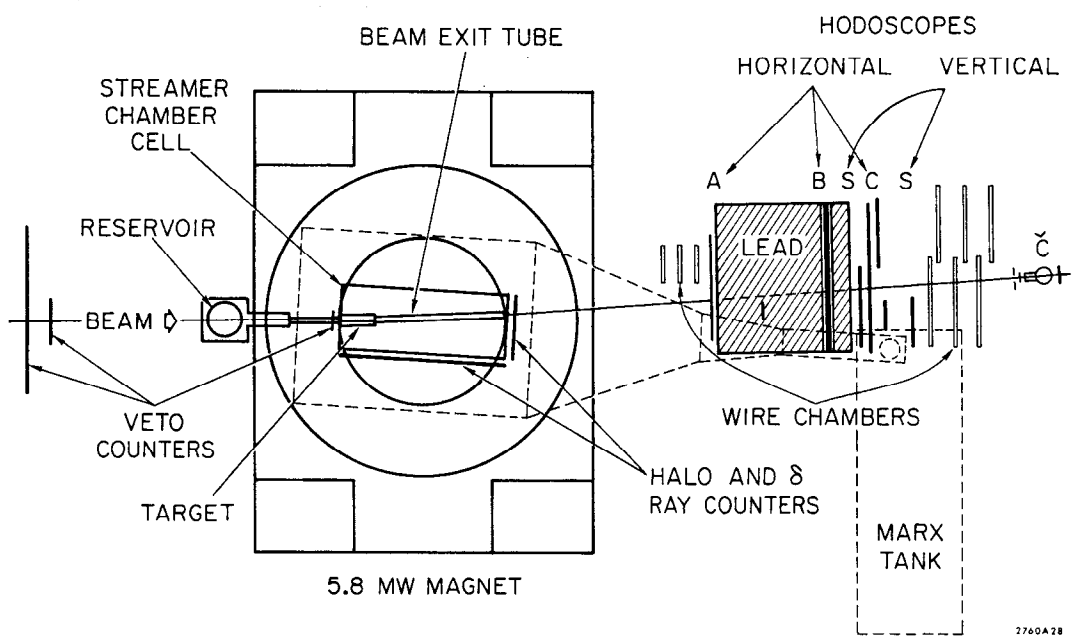

Fig. 1--Streamer chamber experimental configuration.

penetrating a downstream wall of lead 1.5 meters thick. The trigger was designed to be most sensitive to muons interacting by exchange of a virtual photon with a negative mass-squared, Q^2, greater than 0.5 GeV^2. About 6,000 events were obtained with $Q^2 > 0.3$

*Work supported by the U. S. Energy Research and Development Administration.
(Invited paper presented at the International Symposium on Lepton and Photon Interactions, Stanford University, Stanford, California, August 21-27, 1975.)

GeV^2 and lepton energy loss ν greater than 2.0 GeV. The analysis was done in terms of particle production according to the graph shown in Fig. 2. Useful invariants are defined as follows:

$$s \equiv W^2 = 2M\nu + M^2 - Q^2$$

$$\frac{1}{\omega} = -\frac{q^2}{2p\cdot q} = \frac{Q^2}{2M\nu} \qquad z = \frac{p\cdot h}{p\cdot q} = \frac{E_h^{lab}}{\nu} \simeq \frac{p_h^{lab}}{\nu}$$

An additional variable used is

$$x = \frac{p^{cm}_{\parallel\ hadron}}{p^{cm}_{max}}$$

while for e^+e^- annihilation comparisons we use

$$\bar{\omega} = \frac{2q\cdot h}{q^2} = \frac{2E_h}{\sqrt{s}}$$

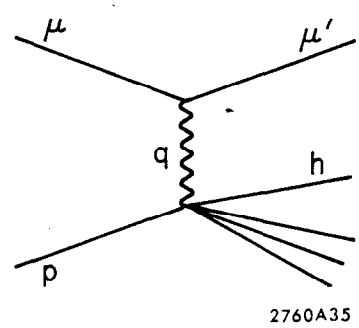

Fig. 2

M is the proton mass, ν the laboratory energy of the photon, E_h^{lab} the laboratory energy of the hadron and $q^2=-Q^2$.

Although most of the data reported are from the "scaling region," $Q^2>0.5$ GeV^2 and $\nu>2$ GeV, comparisons with parton predictions can best be made when not interfered with by the kinematic constraints present in this relatively low energy experiment ($2<\nu<12$). Such constraints are readily apparent in a consideration of the one-prong final states. It is clear that this state must predominate in regions near the kinematic boundary. For example, the ratio, R, of plus-to-minus particles must approach infinity at the boundary. Moreover, the single pion production graph, Fig. 3, is entirely peripheral in character and in conjunction with its associated resonance graphs (to make it gauge invariant) will have little weight in the framework of an analysis in the parton picture. As a result we elect to show some of our data with one-prong events removed. We are aware of the possible bias this may produce but we feel that it may allow the perception of some characteristics of the data otherwise obscured by kinematic considerations. In addition, we have not in this experiment distinguished particle masses; as a result our data on positive particles contain a mixture of protons as well as kaons and pions. In many cases, therefore, we present here data primarily on negative particles.

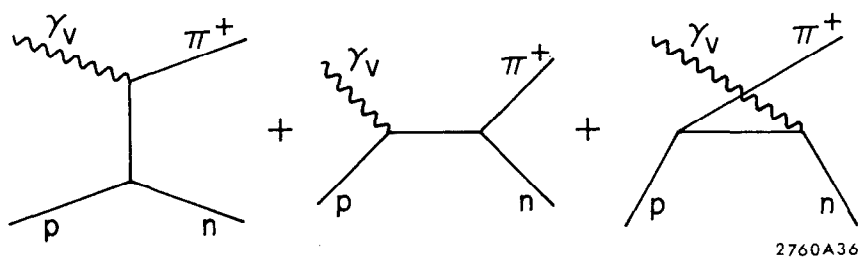

Fig. 3

Although our initial expectation had been to study the effects of Q^2 on hadron production observed in these interactions one must hunt very diligently to find Q^2 effects.

In a study of multiplicity and topological cross sections we find virtually no variation with Q^2 except in the very low Q^2 region below 0.5 GeV^2 where the onset of longitudinal photons may be the cause of differences observed. In Fig. 4 we show the result of our study of average charged hadron multiplicity. The solid curves are our data normalized to the total cross section. These are not incompatible with other published data. The solid squares on the other hand are our data with one-prong events removed. This, of course, yields a higher value of average charged multiplicity which is equal to two times the average number of negatives plus one. A remarkable agreement of this latter multiplicity with that from e^+e^- annihilation (SPEAR, open circle)[1] can be observed.

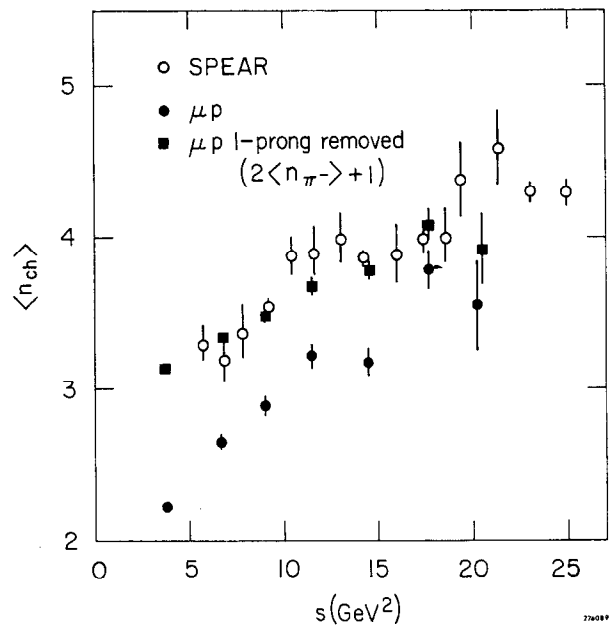

Fig. 4--Average charged multiplicity.

A calculation can be made which indicates that this agreement may be more than fortuitous. In Fig. 5 one compares the diagram of virtual photoproduction on the left with the diagram of e^+e^- annihilation on the right.

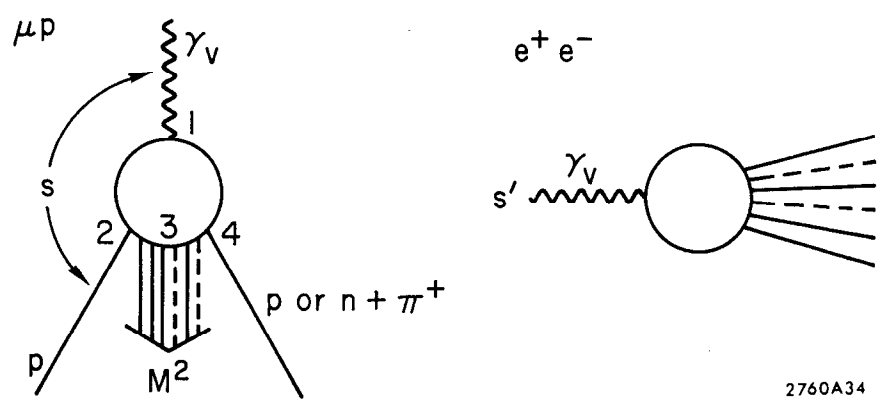

Fig. 5

The following assumptions are made:

A. The average charged multiplicity in the e^+e^- annihilation can be expressed as

$$\langle n \rangle_{e^+e^-} = A \ln \frac{s'}{s_0}$$

B. The multiplicity at vertex 3 in virtual photoproduction is the same as the average multiplicity in e^+e^- annihilation for a value of s' equal to M^2 at vertex 3.

C. The average logarithmic fraction of s carried off at vertex 3 is relatively constant.

The multiplicity at vertex 3 averaged over the distribution function of M^2 yields the following results:

$$\langle n\rangle_{\gamma_v} \simeq \langle n\rangle_{e^+e^-} + 1 + A\int_0^1 \ln(1-x_p)\, f(x_p)\, d(1-x_p)$$

where $x_p = E_p/E_{p\,max}$; E_p is the c.m. energy carried off at vertex 4 and $f(x_p)$ is the distribution function of x_p. If the integral (the logarithmic fraction of s) is constant the variation with s will be the same. Moreover $A \simeq 1$ and if, for example, $f(x_p)$ is constant, $\langle n\rangle_{\gamma_v}$ will approximately equal $\langle n\rangle_{e^+e^-}$.

The argument, with some increase in complexity, can be generalized to a non-logarithmic distribution. Any incident particle can be assumed at vertex 1 if changes are made at vertex 4. In particular, it should be noted that a comparison must be made with one-prong events removed since SPEAR data do not include events corresponding to one prong in μp scattering. The corresponding events at SPEAR would have all neutral final states.

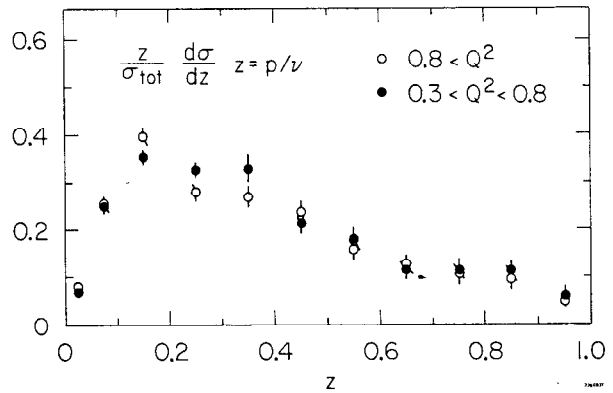

Fig. 6

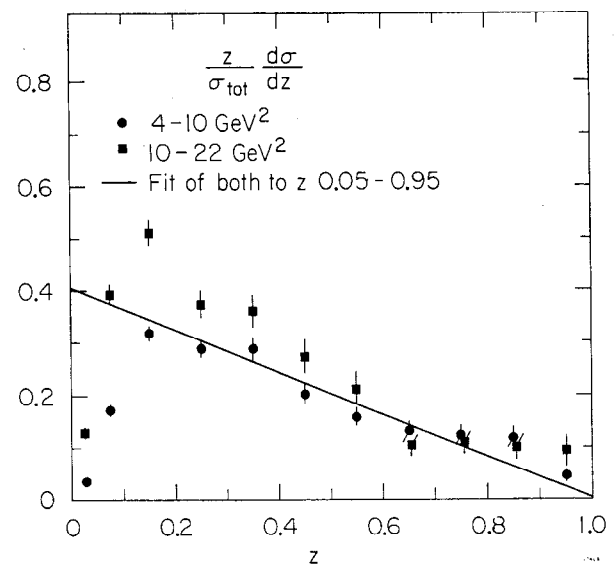

Fig. 7

We pass now to an examination of the hadron structure function. A useful variable in the case of μp scattering is the invariant $z = E^{lab}_{hadron}/\nu$. We use the approximation $z = p_h^{lab}/\nu$, showing the function only for negative particles, since the positive particles may be contaminated by protons. First we show that function for all s values and two Q^2 intervals Fig. 6 shows $(z/\sigma_{tot})(d\sigma/dz)$. Again very little dependence on Q^2 can be observed.

Figure 7 shows the same function integrated over Q^2, in two s intervals. In the normalization used, the total area is equal to the fractional energy carried by negative particles. The straight lines shown are the best fit to (1-z) of points above $z = 0.5$. Figure 8 shows the plot of $(1/\sigma_{tot})(d\sigma/dz)$. The normalization makes the area equal to the negative average multiplicity. The straight line gives the best fit to (1-z) for data points above $z = 0.5$. Obviously any slope can be achieved by a choice of fitted region.

In a different normalization one may examine $(z/\sigma_{\pi^-})(d\sigma/dz)$. Here, the σ_{π^-} signifies the cross section for production of events containing negative pions, that is, one prong events are removed. This is illustrated in Fig. 9. The different energies shown disagree at high z rather than at low z.

Again we compare with SPEAR data. The appropriate comparison is with $(\bar{\omega}/4\sigma_{tot})(d\sigma/d\bar{\omega})$ normalizing to the fractional energy carried by negatives. In e^+e^- data we assume symmetry between positive and negative particles.

The factor of 4 used with the e^+e^- annihilation data is composed of a factor of 2 due to the fact that both π^+ and π^- data are included in the e^+e^- data and only π^- in the μp data.

Another factor of 2 can be justified in either of the following ways:

If data are normalized in such a way that

$$\int_0^1 \frac{\bar{\omega}}{\sigma}\frac{d\sigma}{d\bar{\omega}}\,d\bar{\omega} \quad \text{and} \quad \int_0^1 \frac{z}{\sigma_{\pi^-}}\frac{d\sigma}{dz}\,dz$$

are equal to the average energy fraction carried by negative particles, it is necessary to divide the former by 2 since the fraction of the total event energy expressed by a value of $\bar{\omega}$ is one-half that expressed by the same value of z.

Alternately we can qualitatively argue that the factor is needed since there are 2 leading quarks in e^+e^- annihilation and one in μp scattering.

The e^+e^- hadron functions are remarkably like those of μp and with this normalization have approximately the same area. (See Table I.) It would be interesting to compare at higher s values, where the fraction of energy carried by neutrals has increased appreciably in e^+e^- annihilation.

Table I. Average fractional energy carried by negatives.

	s=9	s=14.4
e^+e^-	0.267 ± .006	0.239 ± .005
	s=4-10	s=10-22
μp	0.291 ± .008	0.281 ± .009

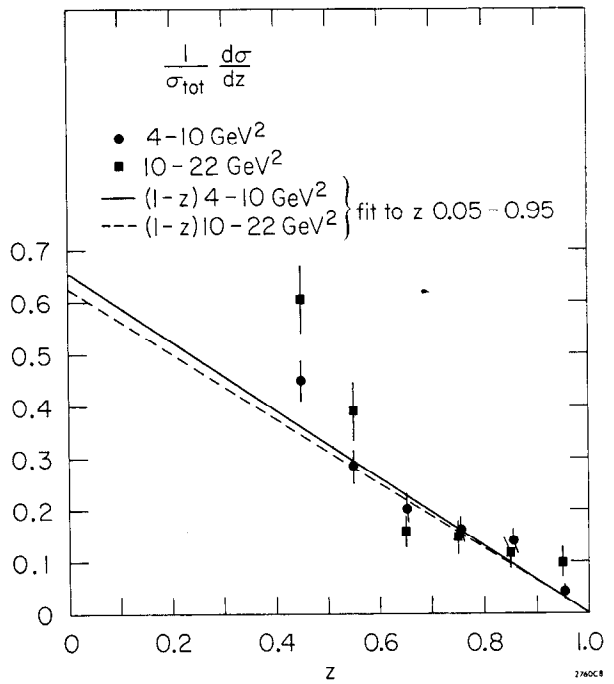

Fig. 8

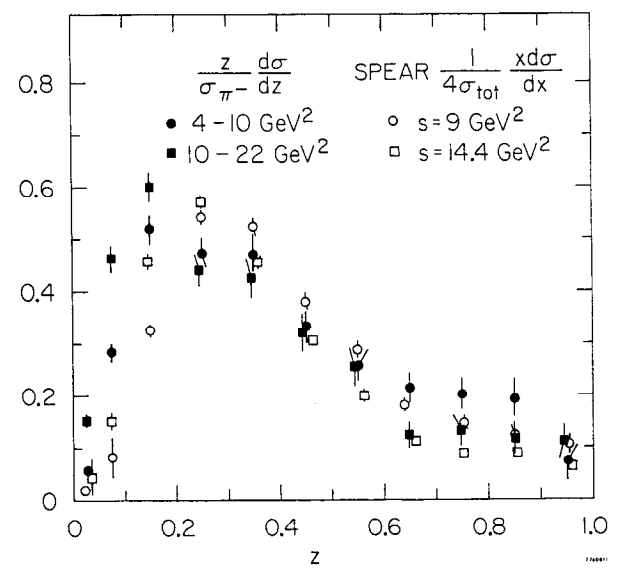

Fig. 9

We are unable to compare the structure functions for positive mesons because of our inability to separate protons from pions and kaons. Figure 10 shows the ratio of

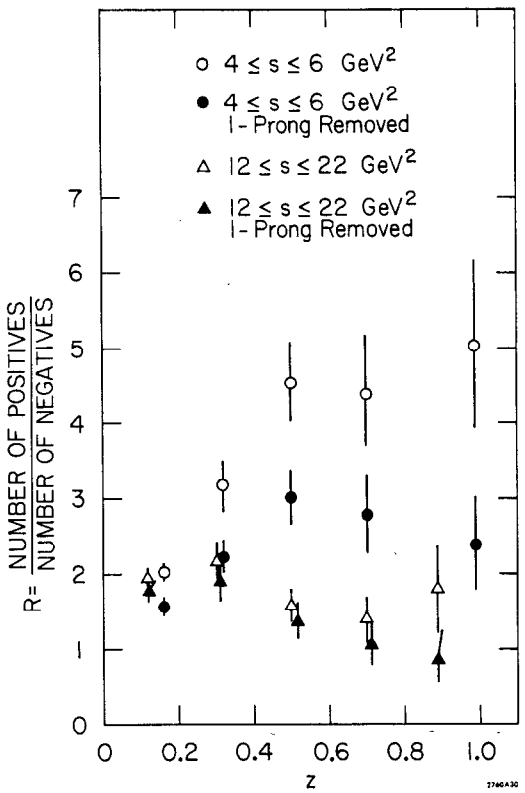

Fig. 10--Ratio of positive to negative particles as a function of z.

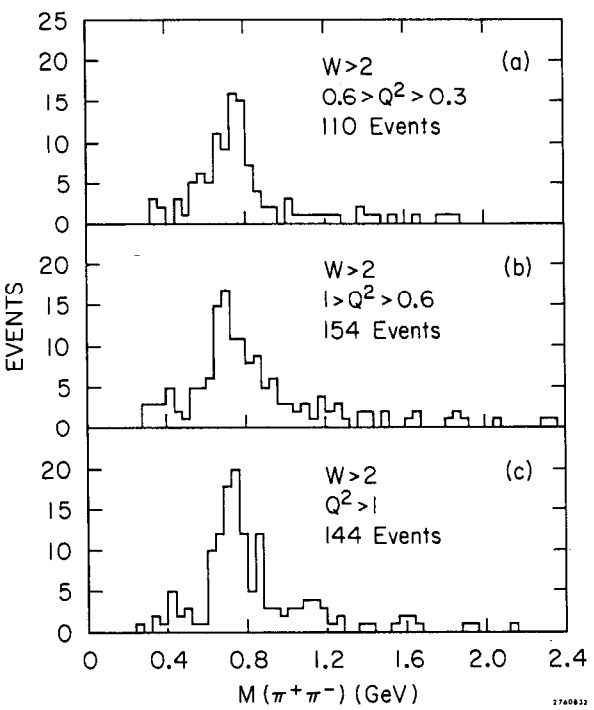

Fig. 11--$\pi^+\pi^-$ mass plots for $\gamma_V p \rightarrow \pi^+\pi^- p$.

the number of positives to negatives as a function of z. At high energy, the high z region should be relatively free of protons; there we see a ratio of $\simeq 2$ if all topologies are used, and $\simeq 1$ if 1-prongs are omitted.

Hence we might continue with positives to have reasonable agreement between μp and SPEAR as long as 1-prong events are removed but certainly no agreement if all topologies are included. Comparisons using the normal hadronic variable $x = p_{\parallel}^{cm}/p_{max}^{cm}$ are at best confusing because of normalization problems, since x goes from -1 to +1 while $\bar{\omega}$ or z goes from 0 to 1.

Exclusive Results

I would like to present a few results on exclusive production. The analysis of ρ^o production is the result of a maximum likelihood analysis of our data on $\gamma_V p \rightarrow \pi^+\pi^- p$, taking into account the Δ^{++} and a phase space background. Since the target region is obscured there are missing particles in about 1/3 of the ρ^o events; we then have 1-C rather than 4-C fits in these cases. The validity of each of these 1-C fits was checked on the scanning table. Figure 11 shows the ρ^o mass peaks observed.

A study was also made of ω meson production using a $\gamma_V p \rightarrow \pi^+\pi^-\pi^o p$ hypothesis for three prong events. (See Fig. 12 for the mass plots.) Here any loss of a charged particle from the reaction makes analysis impossible since there is only one constraint to start with. Corrections were applied by assuming the same loss rate for ω's as for ρ^o's. Hence

$$\omega_{Real} = \omega_{Observed} \times \frac{\rho^o_{1-C} + \rho^o_{4-C}}{\rho^o_{4-C}}$$

The coefficient of a fit to e^{-At} for the ρ^o is given in Fig. 13. There is no evidence for a change of A with Q^2. The fractional ρ^o cross section as a function of Q^2 is shown in Fig. 14. The apparent disagreement between our data and the DESY data[2] may well be due to the difference in energy. However there appears to be some disagreement with

the published value for the SLAC hydrogen bubble chamber experiment.[3] Our ρ^0 data are summarized in Table II.

The results of the ω measurements are summarized in Fig. 15. Again, we

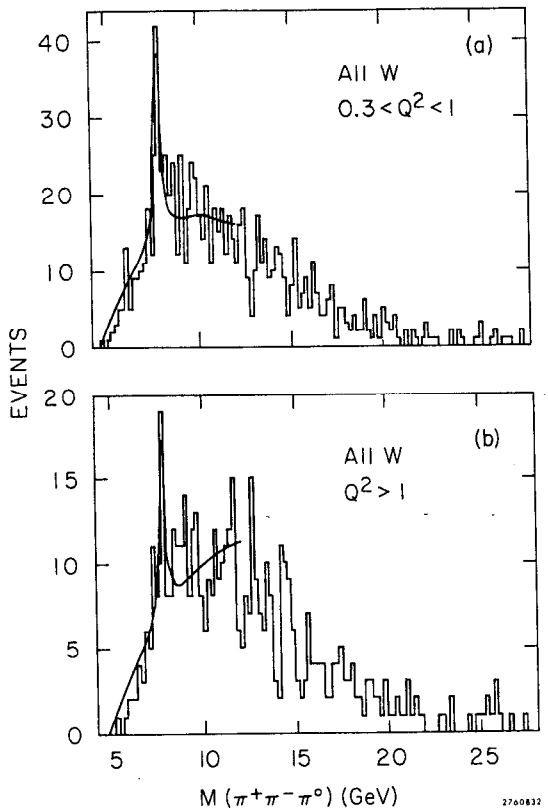

Fig. 12--$\pi^+\pi^-\pi^0$ mass plots for $\gamma_V p \rightarrow \pi^+\pi^-\pi^0 p$.

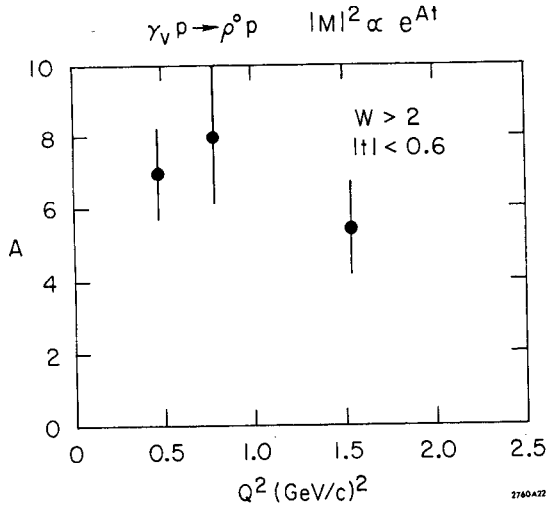

Fig. 13--Exponential t dependence coefficient as a function of Q^2.

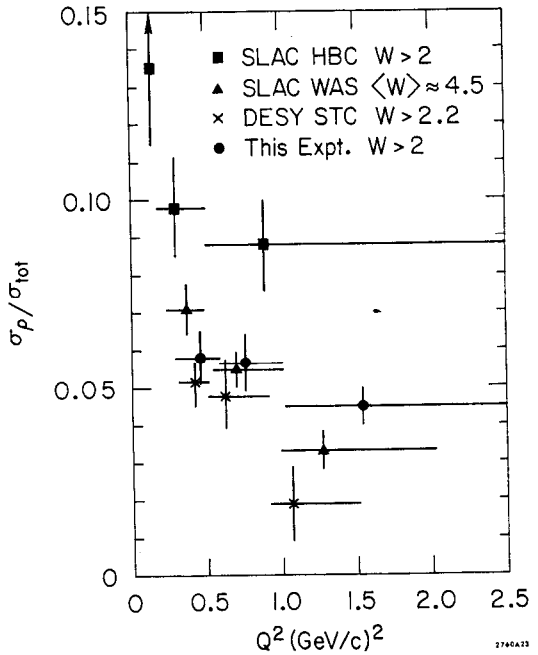

Fig. 14--Fractional ρ^0 cross sections as a function of Q^2.

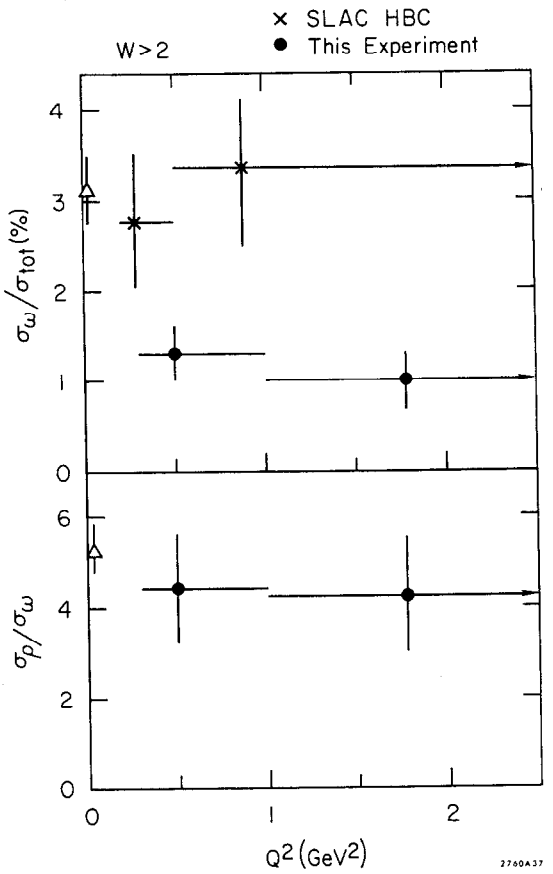

Fig. 15--Fractional ω cross sections as a function of Q^2.

Table II. Cross section results.

W	Q^2	σ_ρ/σ_{tot}	$\sigma_t + \epsilon\sigma_L$ (μb)	σ_ρ (μb)
	.3 - .6	.0742 ± .015	101.8	7.55 ± 1.53
1.7 - 2.0	.6 - 1.	.0762 ± .017	73.68	5.61 ± 1.25
	1.	.0413 ± .016	21.28	.879 ± .340
	.3 - .6	.0544 ± .012	81.84	4.45 ± .958
2.0 - 2.5	.6 - 1.	.0572 ± .014	59.90	3.42 ± .857
	1.	.0612 ± .012	20.79	1.27 ± .252
	.3 - .6	.0590 ± .0094	63.82	3.77 ± .600
2.5 - 4.6	.6 - 1.	.0546 ± .0086	45.85	2.50 ± .394
	1.	.0344 ± .0051	19.28	.663 ± .098
	.3 - .6	.0575 ± .0072	67.30	3.87 ± .518
2.0 - 4.6	.6 - 1.	.0559 ± .0072	48.61	2.72 ± .350
	1.	.0448 ± .0050	19.61	.879 ± .097

find no Q^2 dependence in our region of measurement, but a significant decrease relative to photoproduction. The cross section reported here is significantly lower than that from the SLAC HBC experiment.[3]

Turning now to the decay process, the ρ^0 decay was analyzed in the s channel helicity system (see Fig. 16). θ and ϕ are defined as polar and azimuthal angles of the decay π^+ in the ρ^0 rest frame. θ is measured with respect to the ρ^0 direction of flight while ϕ is the angle between the ρ^0 production plane and the decay plane. ϕ_μ is the angle between the ρ^0 production plane and the μ scattering plane which is the plane of transverse polarization. We plot the decay with respect to θ and to $\psi = \phi + \phi_\mu$.

Figure 17 shows the θ distribution for $\gamma_V p \rightarrow \pi^+\pi^- p$. For ρ^0 production by longitudinal photons there would be a $\cos^2\theta$ distribution with maxima at +1 and -1, while for transverse photons it would be $\sin^2\theta$. The curve shows the result of the maximum likelihood analysis. The enhancement at $\cos\theta = -1$ is due to Δ^{++} production. Figure 18 shows the distribution which relates ρ^0 decay to transverse photons and distinct evidence of an appropriate asymmetry can be seen. As a result of the maximum likelihood analysis we obtain $\sigma_{longitudinal}/\sigma_{transverse}$ as shown in Fig. 19.

Although our data by themselves would not substantiate a rise in $\sigma_{longitudinal}/\sigma_{transverse}$ near Q^2=1, in combination with other data[2-4] some evidence for such an effect is apparent. Moreover, inclusive spectrometer data[5] (Fig. 20) indicate a rise in the total cross section in the same Q^2 region and it may be true that vector meson production contributes to this.

I summarize my report as follows: We find an interesting similarity between our data on charged multiplicity and those for e^+e^- annihilation. An examination of our π^- structure function shows scaling at high z when normalized to the total cross sections. When normalized to the cross section for events containing π^-'s, the structure functions very closely resembles those from e^+e^-.

In our study of vector meson production we find no Q^2 dependence in the production of either the ρ^0 or ω after an initial drop from photoproduction values. Remarkably, the ratio of ρ to ω production appears to remain the same from photoproduction to the

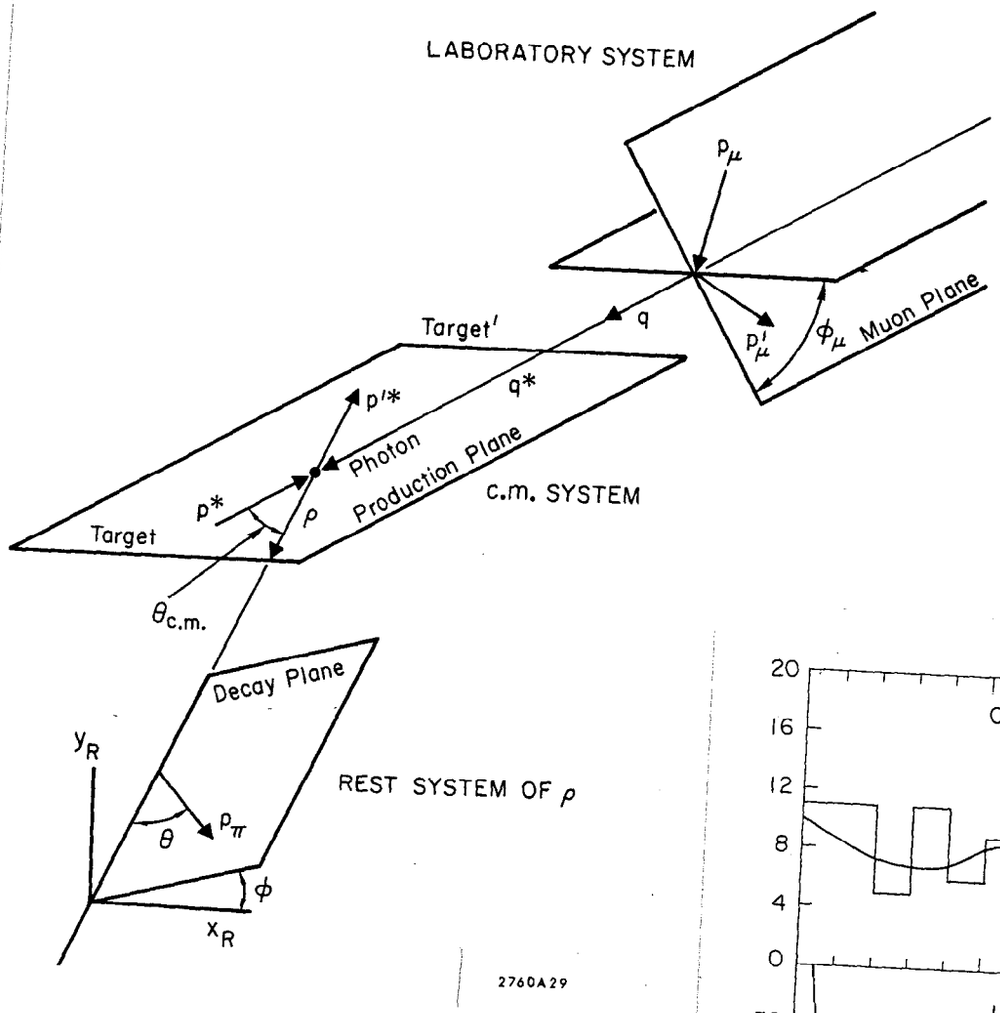

Fig. 16--Angular relations for ρ^o decay analysis.

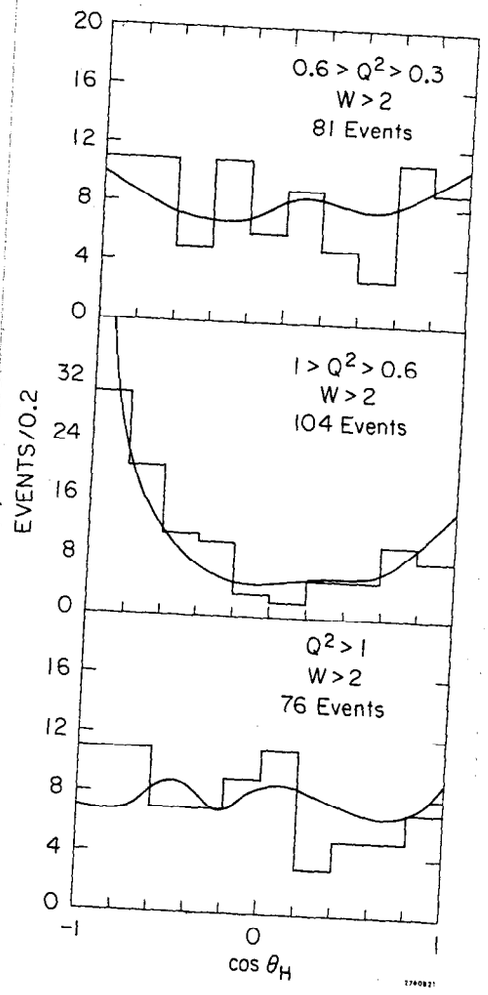

Fig. 17--θ distribution for $\gamma_V p \rightarrow \pi^+\pi^- p$.

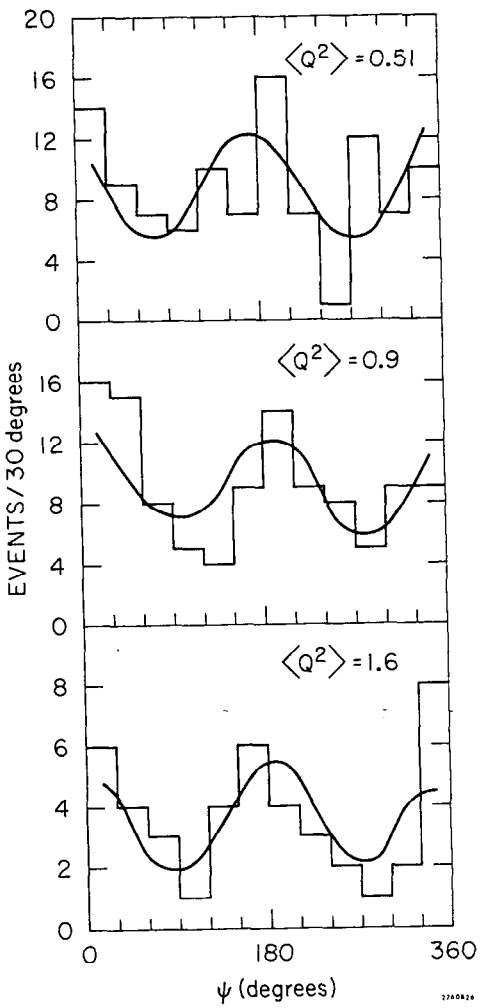

Fig. 18--ψ distribution for $\gamma_V p \rightarrow \pi^+\pi^- p$.

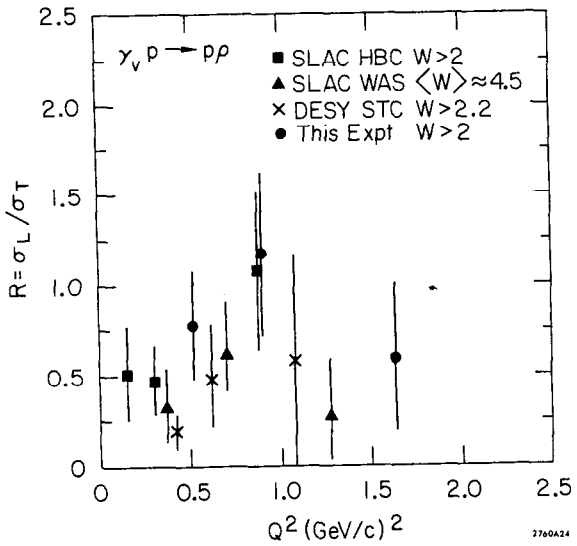

Fig. 19--Ratio of longitudinal to transverse cross section as a function of Q^2 for $\gamma_V p \rightarrow \pi^+\pi^- p$.

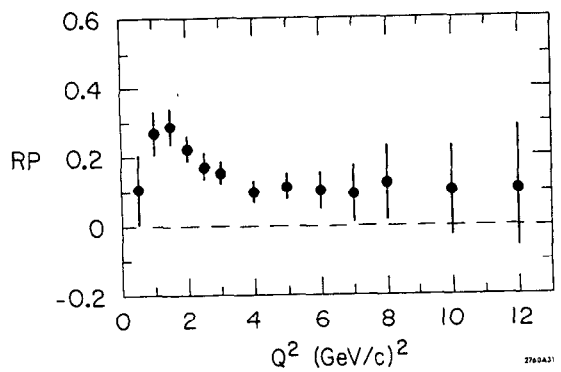

Fig. 20--Inclusive measurement of longitudinal to transverse cross section ratio.

highest Q^2 studied. Our examination of the ratio of $\sigma_{longitudinal}/\sigma_{transverse}$ in ρ^0 production adds evidence for a rise near Q^2=1 and possibly a later drop.

REFERENCES

1. Robert Hollebeck, University of California Berkeley, Ph.D. Thesis, LBL-3874 and M. Perl, private communication.
2. V. Eckardt et al., DESY 74/5 (February 1974).
3. J. Ballam et al., Phys. Rev. D 10, 765 (1974).
4. J. Dakin et al., Phys. Rev. D 10, 1401 (1974).
5. E. M. Riordan, MIT Thesis, MIT Report No. COO-3069-176 (1973).
   E. D. Bloom, Proceedings of the 6th International Symposium on Electron and Photon Interactions at High Energies, p. 227.